

# Nicotine and Carbamylcholine Binding to Nicotinic Acetylcholine Receptors as Studied in AChBP Crystal Structures

Patrick H.N. Celie,<sup>1</sup> Sarah E. van Rossum-Fikkert,<sup>1</sup>  
Willem J. van Dijk,<sup>1</sup> Katjuša Brejc,<sup>1,3</sup>  
August B. Smit,<sup>2</sup> and Titia K. Sixma<sup>1,\*</sup>

<sup>1</sup>Division of Molecular Carcinogenesis  
Netherlands Cancer Institute

Plesmanlaan 121  
1066 CX Amsterdam  
The Netherlands

<sup>2</sup>Department of Molecular and Cellular  
Neurobiology

Institute of Neurosciences  
Faculty of Earth and Life Sciences  
Vrije Universiteit  
De Boelelaan 1085  
1081 HV Amsterdam  
The Netherlands

## Summary

Nicotinic acetylcholine receptors are prototypes for the pharmaceutically important family of pentameric ligand-gated ion channels. Here we present atomic resolution structures of nicotine and carbamylcholine binding to AChBP, a water-soluble homolog of the ligand binding domain of nicotinic receptors and their family members, GABA<sub>A</sub>, GABA<sub>C</sub>, 5HT<sub>3</sub> serotonin, and glycine receptors. Ligand binding is driven by enthalpy and is accompanied by conformational changes in the ligand binding site. Residues in the binding site contract around the ligand, with the largest movement in the C loop. As expected, the binding is characterized by substantial aromatic and hydrophobic contributions, but additionally there are close contacts between protein oxygens and positively charged groups in the ligands. The higher affinity of nicotine is due to a main chain hydrogen bond with the B loop and a closer packing of the aromatic groups. These structures will be useful tools for the development of new drugs involving nicotinic acetylcholine receptor-associated diseases.

## Introduction

Nicotinic acetylcholine receptors (nAChRs) and the structurally related GABA<sub>A</sub>, and GABA<sub>C</sub>, 5HT<sub>3</sub> serotonin, and glycine receptors are well studied, pharmacologically important ligand-gated ion channels (LGICs) in the central and the peripheral nervous system (Karlin, 2002; Le Novère and Changeux, 2001). They consist of homo- or heteropentamers of homologous subunits, with an N-terminal ligand binding domain and a C-terminal transmembrane domain. The extracellular ligand binding domains contain a conserved disulfide pair that forms a so-called Cys-loop, which gives rise to the alternate name of Cys-loop receptors. These domains form

2–5 binding sites at selected subunit interfaces. In response to agonist binding, a single ion channel is opened. LGICs are involved in important aspects of brain functioning, and disease and mutations in these receptors lead to diseases such as congenital myasthenia gravis, epilepsy, alcohol abuse (nAChRs, GABA<sub>A</sub>Rs), or startle syndrome (glycine receptors) (Vafa and Schofield, 1998). Specifically, nAChRs mediate nicotine addiction in tobacco smokers.

Nicotinic receptors are, besides their endogenous ligand acetylcholine, reactive to chemically diverse pharmaceuticals and naturally occurring compounds such as nicotine, alcohol, and various toxins. The ligand binding site is characterized by the presence of aromatic and hydrophobic residues that are contributed by two neighboring subunits and a disulfide bond between two adjacent cysteine residues. The principal subunit provides residues from loops A, B, and C, whereas residues within loops D, E, and F come from the complementary subunit.

Acetylcholine binding protein (AChBP) is a water-soluble protein produced in molluscan glia cells. It functions in modulating the synaptic transmission of acetylcholine (Smit et al., 2001). Because of its high sequence similarity to all LGICs (15%–28% identity), the crystal structure of AChBP (Brejc et al., 2001) is the established model for the extracellular domain of the pentameric LGICs (Cromer et al., 2002; Karlin, 2002; Reeves and Lummis, 2002; Sine, 2002; Sixma and Smit, 2003), and homology models have been generated to analyze receptor-ligand interactions (Le Novère et al., 2002; Schapira et al., 2002). *Lymnaea stagnalis* AChBP has pharmacological properties similar to the homomeric  $\alpha 7$  subtype of the nAChRs, with relatively weak affinity for acetylcholine and  $\sim 10$ -fold higher affinity for nicotine (Hansen et al., 2002; Smit et al., 2001). Here we have determined the crystal structures of AChBP in complex with the nAChR agonists carbamylcholine and nicotine. Both ligands bind at the same position and cause similar local conformational changes within the protein. We have applied isothermal titration calorimetry to determine the affinity of both ligands for AChBP. This allows a thermodynamic analysis of ligand binding to a nAChR homolog. In combination with the atomic resolution binding data, this provides a major step forward in the understanding of the ligand binding parameters of nicotinic acetylcholine receptors.

## Results and Discussion

### Structure Analysis

The crystal structures of AChBP with nicotine (2.2 Å), carbamylcholine (2.5 Å), and HEPES (2.1 Å) were solved from different preparations of protein and crystallized in different space groups (Table 1). The data quality was such that noncrystallographic symmetry constraints were required during refinement, for regions that were structurally invariant between subunits (55%–75%). Because of the high redundancy (10–20 subunits per asym-

\*Correspondence: t.sixma@nki.nl

<sup>3</sup>Present address: Cytokinetics, South San Francisco, California.

Table 1. Crystallographic Parameters

	HEPES	Carb <sup>a</sup>	Nic <sup>b</sup>
Space group	P4 <sub>1</sub> 2 <sub>1</sub> 2	P4 <sub>3</sub> 2 <sub>1</sub> 2	P2 <sub>1</sub> 2 <sub>1</sub> 2
Resolution (Å)	50–2.1	50–2.5	50–2.2
Redundancy	13.4	12.8	8.0
R <sub>merge</sub> (%)	11.1	12.3	9.4
I/σI	10 (1.3)	13 (2.8)	9 (1.7)
Complete (%)	99 (99)	96 (98)	86 (38)
Refinement			
Resolution (Å)	12–2.1	12–2.5	12–2.2
Reflections	127,031	76,092	184,182
Atoms	18,194	16,488	34,792
R factor (%)	23.6	22.8	22.4
R <sub>free</sub> (%)	28.4	26.4	26.5
Rms bonds (%)	0.012	0.015	0.015
Rms angle (°)	1.32	1.46	1.46

<sup>a</sup> Carbamylcholine bound to AChBP.<sup>b</sup> Nicotine bound to AChBP.

metric unit), the resulting structures are convincing but do not optimally address subtle changes between subunits.

In the nicotine bound structure, the ligand has well-resolved electron density in all 20 subunits in the asymmetric unit. In contrast, carbamylcholine could only be built in 3 of the 10 sites. It is apparent from the electron density maps that the other sites are not completely empty. These subunits probably contain solute molecules, but due to the limited resolution we have not been able to resolve them. The three sites with carbamylcholine bound agree well with each other and indicate that there is only a single binding mode. The other subunits resemble the HEPES bound conformation. The lower number of sites filled with carbamylcholine compared to nicotine may be due to the lower affinity of carbamylcholine for AChBP (Table 2) or to the variation in crystallization condition (see Experimental Procedures).

Both structures are compared to a high-resolution HEPES bound structure (2.1 Å), since ligand-free crystals did not yield interpretable data. A HEPES molecule was resolved in 3 of the 5 binding sites of each pentamer, but the orientation of HEPES in one site is distinct from the other two (see Supplemental Figure S1 at <http://www.neuron.org/cgi/content/full/41/6/907/DC1>). Both HEPES orientations had previously been observed (Brejc et al., 2001; Sixma and Smit, 2003), but only at this resolution could they be resolved. A fourth binding site has an ammonium sulfate molecule bound, whereas density in the fifth site could not be resolved.

Table 2. Thermodynamic Parameters of AChBP-Ligand Interaction

Ligand	K <sub>d</sub> (nM)	ΔH (kcal mol <sup>-1</sup> )	-TΔS (kcal mol <sup>-1</sup> )
Car <sup>a</sup>	7575 ± 431	-13.4 ± 0.4	6.46 ± 0.57
Ach <sup>b</sup>	823 ± 40	-12.5 ± 0.1	4.23 ± 0.32
Nic <sup>c</sup>	45.2 ± 2.3	-14.5 ± 0.2	4.52 ± 0.14

Isothermal titration calorimetry was performed in 100 mM NaCl and 25 mM sodium phosphate buffer (pH 8.0).

<sup>a</sup> Carbamylcholine.<sup>b</sup> Acetylcholine.<sup>c</sup> Nicotine.

### Ligand Binding

As expected, the ligands are bound in the interface between subunits (Figure 1; for reviews, see Arias, 2000; Corring et al., 2000; Karlin, 2002; Sine, 2002). They make contact on the principal (+) side with residues from loops A, B, and C that are particular to α subunits in nicotinic receptors. The complementary (-) binding side delivers the more variable modulating residues in loops D and E, as found in, for example, the γ and δ subunits in the muscle receptor. The ligands are completely buried by the protein. There are more direct contacts with the principal side (Figure 2), burying about 75 and 70 Å<sup>2</sup> for nicotine and carbamylcholine, respectively, than from the complementary side, which buries 50 and 36 Å<sup>2</sup>, respectively.

On the principal side, the ligands make extensive aromatic contacts with the Trp143 side chain (Galzi et al., 1991; Zhong et al., 1998) and some with Tyr192 (Middleton and Cohen, 1991; O'Leary and White, 1992). Tyr185 contributes aromatic contacts to the choline binding as expected (Middleton and Cohen, 1991; O'Leary and White, 1992; Sine et al., 1994), but hardly interacts with nicotine, which explains why a mutation at this site affects nicotine binding much less than acetylcholine binding (Galzi et al., 1991). There are no aromatic contacts to Tyr89, but its hydroxyl group has a close contact with the ligand. This interaction is consistent with the strongly reduced affinity for acetylcholine and carbamylcholine of Tyr to Phe mutant nAChR's at this position (Sine et al., 1994). The close proximity of Tyr89 to the trimethylammonium group in carbamylcholine explains why labeling with acetylcholine mustard specifically alkylates the equivalent Tyr93 in the *Torpedo* α subunit (Cohen et al., 1991). The vicinal disulfide is in contact with the ligands, mostly through Cys187 with carbamylcholine and through Cys188 with nicotine. These contacts clarify why the vicinal disulfide could not be reduced after agonist binding (Damle and Karlin, 1980).

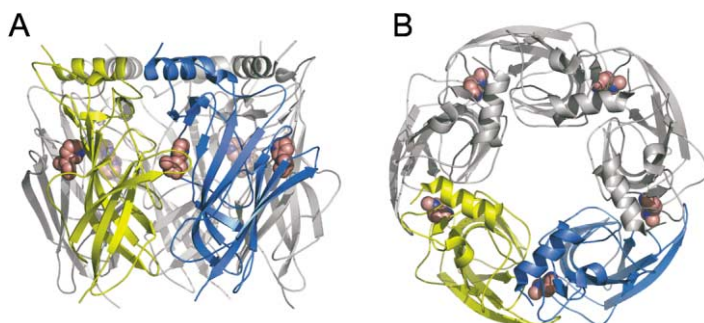


Figure 1. Pentameric AChBP Bound to Nicotine

(A) Schematic representation of AChBP with nicotine (pink) bound. One subunit in yellow, one in blue, view with membrane at the bottom in nAChRs.

(B) Orthogonal view of (A), toward the membrane in nAChRs.

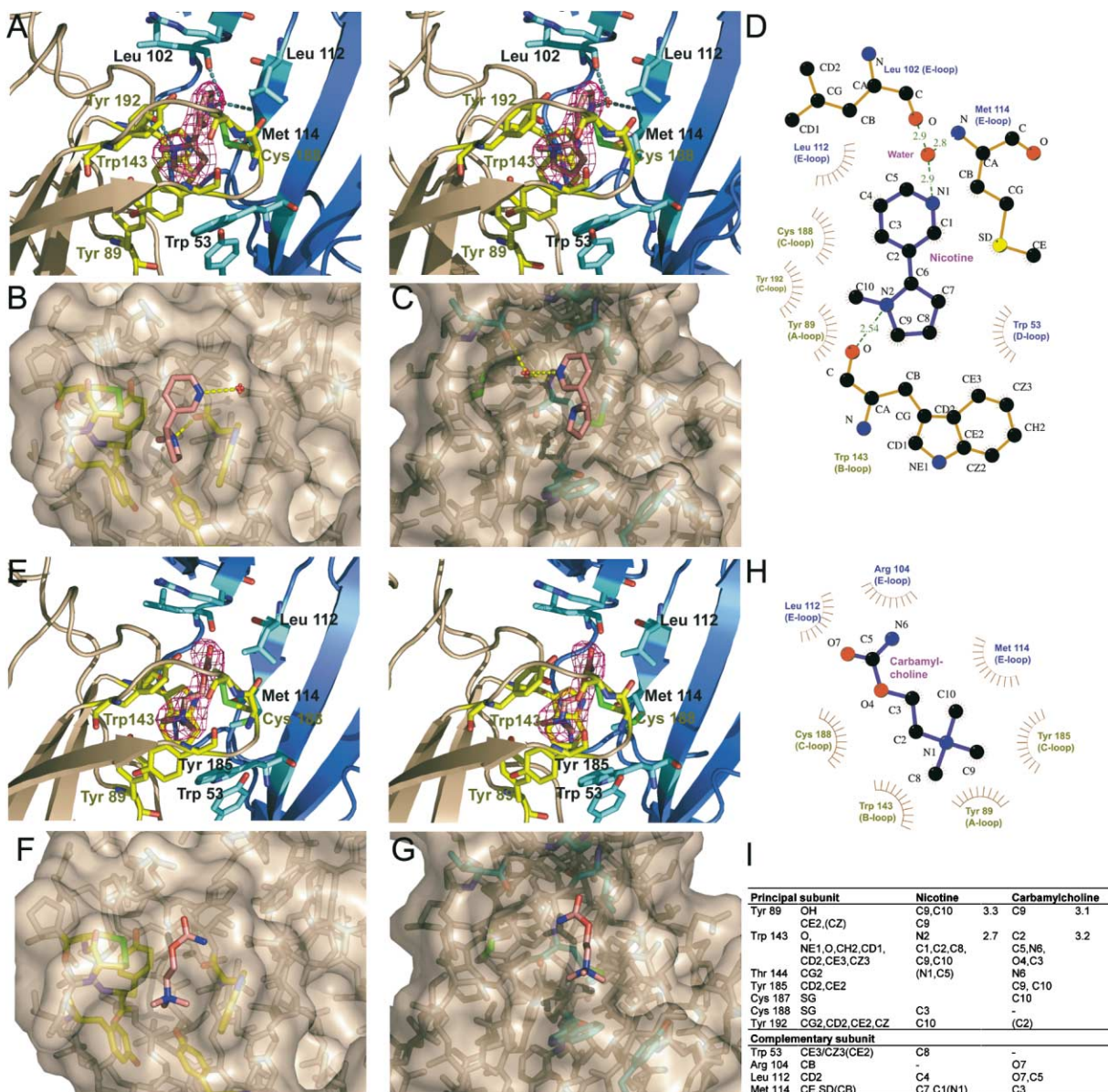


Figure 2. Nicotine and Carbamylcholine Binding to AChBP

(A) The nicotine binding site shown in stereo, ligand in ball-and-stick, with electron density (SigmaA weighted) superimposed, and residues in the binding site in yellowish (principal side) and blueish (complementary side).

(B and C) The opened-up binding site is shown as surface representation for the principal side (B) and the complementary side (C), respectively, with underlying side chains in coloring scheme of (A).

(D) Schematic ligand interactions of nicotine showing hydrogen bonds and van der Waals contacts.

(E-H) Carbamylcholine binding is shown in stereo (E), surface representation in opened-up binding site (F, G), and schematic figure (H).

(I) The interacting atoms (cut-off 3.9 Å) are tabulated. Contacts are shown when present in the majority of subunits, in brackets when present less than half the subunits. Distances are shown if less than 3.3 Å.

On the complementary side, Trp53 makes limited aromatic contacts to nicotine, as suggested by mutagenesis studies (Xie and Cohen, 2001). Leu112 and Met114 contribute hydrophobic contacts to the binding of both ligands, while Arg104 only contacts carbamylcholine.

In addition to these hydrophobic and aromatic contacts, two hydrogen bonds contribute significantly to the binding of nicotine. The first hydrogen bond is between the pyridine N1 through a bridging water molecule to the main chain of residues Leu102 and Met114 (Figure 2). There has been much debate about the optimal in-

ternitrogen (N-N) distance in the nicotinoid pharmacophore for maximal binding affinity (Glennon and Dukat, 2000). The observed N1-N2 distance of  $4.4 \pm 0.1$  Å and N2-water distance of  $6.7 \pm 0.1$  Å in our structure are close to the optimal N-N distances of 4.6 and 6.3 Å that have been proposed for these compounds (Abreo et al., 1996). Based on the structure, we suggest that some ligands with the longer N-N distance could position their second nitrogen in the place of the water molecule, to make direct contact with the protein main chain.

The second nicotine hydrogen bond is between the

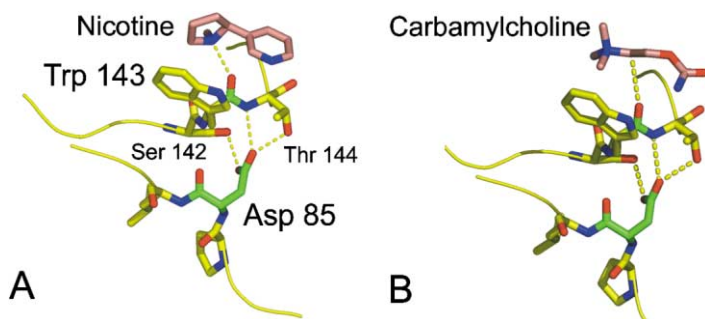


Figure 3. Contribution of Asp85 to Ligand Binding

The charge compensation of (A) nicotine (pink carbons) and (B) carbamylcholine (pink carbons) could be aided by the stabilization of the Trp143 carbonyl oxygen by an Asp85 (green) charged hydrogen bond. The yellow dashed lines indicate the hydrogen bonds.

pyrrolidine N2 and the carbonyl group of Trp143. This carbonyl group is buried by carbamylcholine as well, with a short contact (3.1 Å) to the C2 atom of the positively charged choline group. Such short carbonyl-choline contacts occur frequently in the Cambridge Crystal Structure database (CSD) and are determined by the electrostatic nature of the CH and O atoms, as well as their neighboring atoms (Taylor and Kennard, 1982). Apparently, the positively charged nitrogen N1 in carbamylcholine lowers the electron density around the C2H atoms, which then facilitates the interaction with the carbonyl oxygen to form a CH-O hydrogen bond. Thus, for both nicotine and carbamylcholine, the Trp143 carbonyl group is important for contacting the positively charged group of the ligand.

Upon analysis of this carbonyl group, we noted that it is stabilized by a hydrogen bond between the 143/144 peptide bond NH and the negatively charged Asp85 side chain (Figure 3). This aspartate is conserved throughout the LGIC superfamily and it clearly has a structural role. In addition, however, it may polarize the Trp143 carbonyl oxygen to provide a partial negative charge that favorably interacts with the positively charged group in the ligand. The compensation of nicotinic ligand charge has been extensively debated. One option is that this is accomplished by cation- $\pi$  interactions with aromatic side chains (Zhong et al., 1998). In the structure, these are mainly contributed by Trp143, although residues Tyr192 and either Tyr185 or Trp53 may contribute. However, we suggest that the observed interaction with the partially charged carbonyl of Trp143 may also contribute to charge compensation.

### Comparison of Affinities

Superposition of AChBP bound by nicotine and carbamylcholine shows that these ligands bind similarly, with their nitrogen atoms at almost the same position (Figure 4B). Binding of both ligands is coupled to identical conformational changes (Figure 4 and below), but in binding studies using competition assays (Smit et al., 2001) and ITC (Figure 5, Table 2), there is a 100-fold difference in affinity. In agreement with fluorescence data (Hansen et al., 2002), only a single binding site could be fitted, indicating that there is no cooperativity in AChBP. Surprisingly, the observed stoichiometry (mol ligand/mol pentamer) is reproducibly around 2.5 for carbamylcholine, 3.0 for nicotine, and 5.0 for acetylcholine. Alternative fitting models with multiple sites were not able to explain this. However, it does not affect the more informative thermodynamic parameters: energy for all three

ligands binding is mostly supplied by the change in enthalpy (Table 2). The binding enthalpy reflects the strength of the interactions (e.g., hydrogen bonds, van der Waals contact) and because it is easier to model enthalpy changes, the ligand bound structures may be particularly useful for drug design.

The gain in enthalpy of nicotine versus carbamylcholine binding can be explained by the presence of the hydrogen bonds to nicotine and to the larger number of contacts with the protein for nicotine ( $27 \pm 3$ ) than for carbamylcholine ( $19 \pm 4$ ). Moreover, the burial of the Trp143 carbonyl by carbamylcholine is unfavorable, because it prevents hydrogen bond formation with, for example, water. Entropy changes are generally composed of two terms: a favorable term that reflects the desolvation of water molecules upon burial of hydrophobic residues and an unfavorable term due to loss of flexibility upon ligand binding. Because the local conformational changes in AChBP are similar upon binding of either ligand, the more unfavorable entropy contribution for carbamylcholine binding is probably due to a stronger reduction in conformational freedom of carbamylcholine itself compared to that of nicotine. All these effects together may explain the lower affinity for carbamylcholine and acetylcholine when compared with nicotine. Carbamylcholine binds with 10-fold less affinity than acetylcholine (Table 2), although it differs only by the replacement of the NH<sub>2</sub> group (N6) by a methyl group. Since the N6 is not involved in hydrogen bonds, a methyl group would be energetically more favorable in this hydrophobic environment.

Ligand binding to nAChRs has been modeled for acetylcholine and nicotine (Le Novère et al., 2002; Schapira et al., 2002) based on the (HEPES bound) AChBP crystal structure (Brejc et al., 2001). The acetylcholine models correspond reasonably well with the experimental carbamylcholine position. The nicotine model of Schapira is particularly good because it includes the hydrogen bonds, including those of the bridging water molecule. However, all models lack the rearrangements of the protein that we observe and therefore the detailed contacts are incorrect. Thus, these models are not very good in predicting novel ligand interactions.

In nAChRs there is a variable affinity for these agonists. Alignment of AChBP with nAChRs shows that residues from the principal subunit involved in ligand binding are generally conserved, whereas the residues in the complementary part of the binding site show more variation. For instance, nicotine binds with very high affinity to the  $\alpha_4\beta_2$  receptor subtype. The major differ-

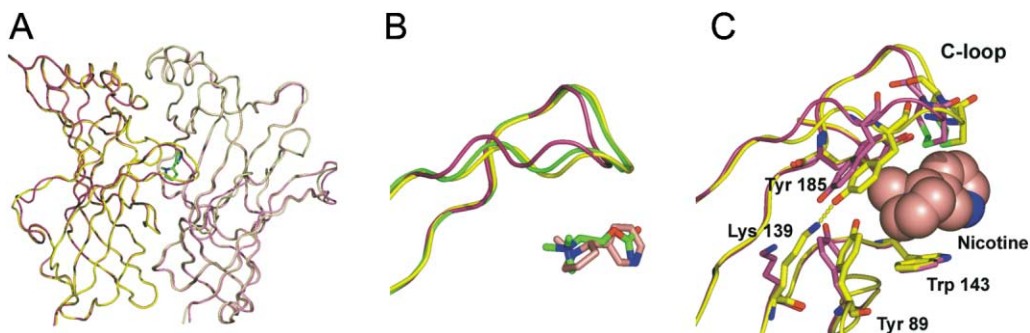


Figure 4. Structural Comparisons between Ligand and HEPES Bound AChBP

(A) Superposition of the backbone of AChBP with HEPES (purple shades) and nicotine (yellow shades) bound; only the C loop and the F loop changing conformation substantially. Nicotine is green.

(B) C loop backbone in HEPES bound (purple), carbamylcholine bound (green), and nicotine bound (yellow) structures. Carbamylcholine (green) and nicotine (pink) shown for their similarity of nitrogen positions.

(C) Comparison of the principal binding side of the nicotine bound (yellow) and HEPES bound (purple) structure, showing the shifts in the C loop and Tyr89 side chains. Nicotine (pink) in space-filling representation. The Tyr185-Lys139 hydrogen bond (yellow dashed line) that is formed upon ligand binding is indicated.

ences between AChBP and  $\alpha_4\beta_2$  in the binding site are the exchange of Arg104 by Val109, Leu112 by Phe117, and Met114 by Leu119. These branched side chains could make better contact with the nicotine carbons. However, analysis of nAChR mutants including chimeric receptors indicates that more remote regions also contribute to affinity (Martin et al., 1996; Osaka et al., 1998; Parker et al., 2001; Prince and Sine, 1996). These effects could be due to small changes in the relative orientation of the subunits.

#### Conformational Changes upon Ligand Binding

Ideally, ligand-induced conformational changes should be analyzed through comparison with a ligand-free structure, but we only have the HEPES bound state. Superposition of the ligand and HEPES bound AChBP

pentamers showed that ligand binding does not alter the relative orientation of the subunits within each pentamer. A series of local conformational changes compared to the HEPES bound structure that were similar for all ligand bound sites was observed. Analysis of the main chain differences with an error-scaled procedure (Schneider, 2002) indicates that only the C loop makes significant backbone movements (Figures 4A and 4B). Although the F loop shows variation in backbone position as well, the electron density is too weak to draw conclusions. In addition to these main chain movements, all side chains in the binding site, with the exception of Trp143, are rearranged to accommodate binding, closing in on the ligand (Figure 4C; Karlin, 2002). The most extensive movements besides the C loop are in the Tyr89 side chain.

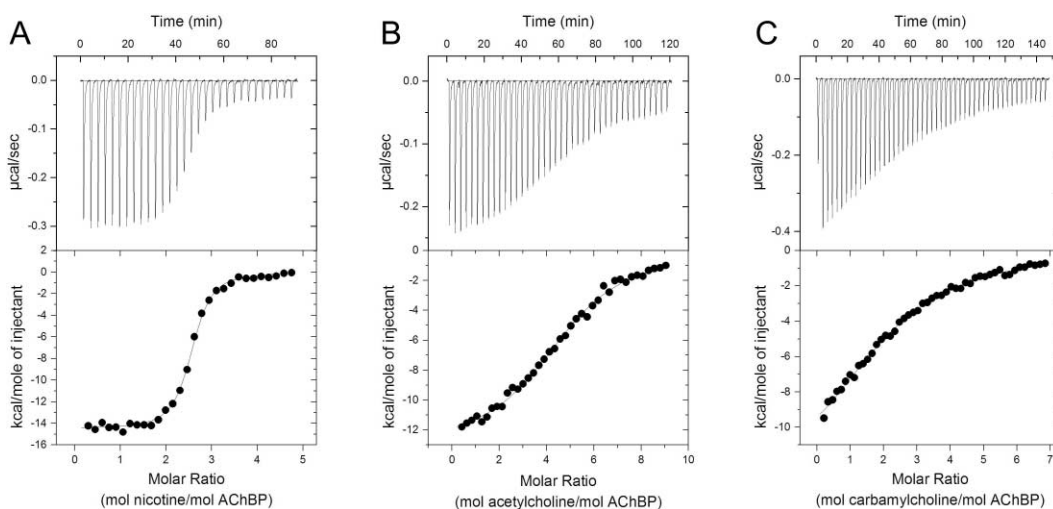


Figure 5. Calorimetric Data of Ligand Binding to AChBP

The top panels show the raw heat measured over a series of injections of (A) nicotine (100  $\mu$ M) into AChBP (2  $\mu$ M), (B) acetylcholine (100  $\mu$ M) into AChBP (3  $\mu$ M), and (C) carbamylcholine (350  $\mu$ M) in AChBP (8  $\mu$ M). Each heat signal is integrated and shown as data point in the bottom panels. Data points were fitted to a model describing a single set of binding sites and best-fit parameters for nicotine, acetylcholine, and carbamylcholine binding were calculated using nonlinear least-squares fitting.

Table 3. Effect of HEPES Binding on AChBP-Nicotine Interaction

Buffer	$K_d$ (nM)	$\Delta H$ (kcal mol <sup>-1</sup> )	$-T\Delta S$ (kcal mol <sup>-1</sup> )
Phosph <sup>a</sup>	45.2 ± 2.3	-14.5 ± 0.2	4.52 ± 0.14
TRIS	64.5 ± 0.6	-12.2 ± 0.5	2.43 ± 0.51
HEPES	265 ± 21	-8.46 ± 0.09	-0.44 ± 0.63

Binding of nicotine to AChBP was performed in 100 mM NaCl and 25 mM of the indicated buffer at pH 8.0.

<sup>a</sup>Sodium Posphate.

There are some additional side chains on the surface that change conformation in the ligand bound state, but most of these vary between subunits. However, in both ligand bound structures, the Lys139 side chain moves systematically to form a hydrogen bond to the hydroxyl group of Tyr185 (Figure 4C). The equivalent hydroxyl group in the nAChR  $\alpha$  subunit (Tyr190) is critical for acetylcholine binding affinity (Sine et al., 1994), channel gating (Galzi et al., 1991), and desensitization (Sine et al., 1994). The Lys139-Tyr185 hydrogen bond could be important because it may affect the ligand affinity, through reorienting the Tyr185 side chain or by stabilizing the C loop conformation in its binding conformation. However, it could also play a role in gating the ion channel, because Lys139 is strictly conserved in the nAChR  $\alpha$  subunits and is located close to the Cys-loop. Formation of the Lys139-Tyr185 hydrogen bond may transduce a change in the Cys-loop that could be part of the channel opening mechanism. Interestingly, the change in the C loop conformation leads to an increased similarity of this loop to the high-affinity peptide (HAP) that has been cocrystallized with  $\alpha$ -bungarotoxin (rms of AChBP residues 182–193 and the HAP peptide is 0.47 Å compared to 0.76 Å previously) (Harel et al., 2001). Extending this to the  $\alpha$ -bungarotoxin position would bring the toxin further into the binding site and changes the relative orientation of toxin and receptor. However, this reorientation hardly affects the contacts between toxin and receptor.

In AChBP, we do not observe any changes that could directly explain the gating process. There is no evidence for systematic rigid body movements as seen in the nicotinic receptor (Unwin et al., 2002). Also, the  $\beta 1/\beta 2$  loop (Glu43-Asn46), which could contact the M2 helix in the transmembrane domain, does not show conformational changes (Miyazawa et al., 2003). This may be because AChBP lacks a transmembrane domain but it could also be because we use the HEPES bound AChBP structure for comparison instead of the true “ligand-free” state. To address whether HEPES binding has an effect on the conformation of AChBP, we compared the thermodynamic parameters of nicotine binding to AChBP in phosphate buffer to those in TRIS and HEPES buffer. The affinity of nicotine for AChBP is about 6-fold lower in the presence of HEPES and, like in phosphate buffer, binding is predominantly determined by the change in enthalpy (Table 3). However, nicotine induces almost no entropy changes in the presence of HEPES, suggesting that HEPES may already alter the conformation of the “empty AChBP” to some extent. The fact that we have difficulties in obtaining a ligand-free AChBP crystal structure also supports the existence of structural alterations between the HEPES bound and the ligand-free state.

Despite the absence of conformational changes that could provide insight in the molecular mechanism of ligand-induced gating, these high-resolution structures reveal agonist binding to a pentameric ligand-gated ion channel, one of the most important classes of drug targets. The binding observed in AChBP is most likely completely identical to that in the  $\alpha$  subunits of the nicotinic receptors and begins to explain the modulatory roles of the complementary subunits. It resolves the various models of nicotine and acetylcholine binding and provides novel explanations for important issues on both the receptor and the ligand side by addressing hotly debated issues such as the charge compensation and the internitrogen distance in the nicotinoid pharmacophore. In the past 2 years the AChBP structure was found to be very informative for interpreting data on other members of the superfamily such as the 5HT<sub>3</sub>, GABA<sub>A</sub>, and glycine receptors (Cromer et al., 2002; Reeves and Lummis, 2002). Most likely, therefore, the increase in knowledge of ligand binding to the nicotinic receptors at high resolution will also provide critical information concerning drug design targeted to other pentameric ion channels.

## Experimental Procedures

### Protein Preparation

AChBP protein was overexpressed in yeast *Pichia pastoris* and purified as described (Brejc et al., 2001). From the crystal structure of AChBP bound to HEPES, it became apparent that oligosaccharides at Asn66 contribute to crystal contacts between pentamers. We speculated that removal of these glycosyl groups could alter the crystal packing. AChBP was incubated o/n with Endo-F1 at room temperature to cleave off the sugar residues, leaving one N-acetylglucosamine attached to the asparagine. Deglycosylated AChBP was subsequently purified by gel filtration (Superdex 200), and the removal of glycosyl groups causing a reduction in molecular weight was confirmed by SDS-PAGE (data not shown). A baculovirus expression system for AChBP was set up to improve protein production. The *Lymnaea stagnalis* AChBP gene including its signal sequence was cloned into the pFastbac I vector. Secreted AChBP was purified by anion exchange (Q-sepharose), gel filtration (Superdex 200), and Mono Q-sepharose and concentrated to 10 mg/ml. Mass spectrometry analysis was performed as described (Smit et al., 2001) and revealed a single molecular species of Mr 24,848. The calculated mass is 23,383, suggesting that a core pentasaccharide of Mr ~1,014 is attached to Asn66. Purity of proteins was estimated to be >99%, as judged by SDS-PAGE and Coomassie blue staining. The pentameric state of purified AChBP was confirmed by size exclusion chromatography, analytical ultracentrifugation (for AChBP purified from *Pichia pastoris*), and static light scattering analysis (for AChBP purified from Sf9 insect cells). No significant differences in ligand binding affinity were measured between AChBP preparations purified from insect cells, yeast, and deglycosylated AChBP when analyzed in a competition assay with [ $\alpha$ -<sup>125</sup>I]bungarotoxin as described previously (Smit et al., 2001).

### Crystallization

Crystals of AChBP grew at room temperature using the hanging drop method. Recombinant AChBP purified from yeast and insect cells as well as deglycosylated protein preparations were all used for crystallization experiments in the presence and absence of ligands. Crystallization conditions were different for native and ligand bound protein, but did not depend on protein preparation. Tetragonal crystals (P4<sub>2</sub>,2) of native AChBP purified from *Pichia pastoris* were grown in a solution of 1.4 M ammonium sulfate, 1% polyethylene glycol (PEG) 200, and 0.1 M HEPES (pH 7.0). Cell constants are: a = b = 140.64 Å, c = 238.26 Å, and 2 pentamers per asymmetric unit (asu). There were 110 atoms found for HEPES and ammonium sulfate

molecules. A total of 140 atoms that are part of glycosyl groups attached to Asn66 could be built in the electron density. All cocrystals were grown using 0.1 M Tris (pH 8.0) instead of HEPES. AChBP (10 mg/ml) was preincubated with 0.8 mM nicotine or carbamylcholine chloride for 2 min before drops were set up. The orthorhombic crystal form (P2<sub>1</sub>2<sub>1</sub>2), a = 232.99 Å, b = 267.41 Å, c = 73.14 Å, 4 pentamers per asu) of deglycosylated AChBP bound to nicotine were grown from 2.1 M ammonium sulfate, 1% PEG200, and 0.1 M Tris (pH 8.0). Within all 20 ligand binding sites in the asu, a nicotine molecule could be built (240 atoms in total). Tetragonal crystals (P4<sub>3</sub>2<sub>1</sub>2) of carbamylcholine bound to AChBP purified from Sf9 insect cells were grown at 2.0 M ammonium sulfate and 0.1 M CAPS (pH 10.5) with cell parameters: a = b = 140.90 Å, c = 240.41 Å and 2 pentamers per asu. Three carbamylcholine molecules (10 atoms each) could be built in the electron density. For all three crystals, the mosaicity was 0.5%.

#### Structure Solution and Refinement

We collected data at ID14 EH4 at the ESRF (Grenoble, France). MOSFLM (CCP4, 1994) was used for indexing of data and designing the optimal data collection strategy. Data were processed and scaled using DENZO and SCALEPACK (Otwinowski and Minor, 1997).

Programs in the CCP4 suite were used to build and refine the models. Initial models of native and ligand bound AChBP were built with the AMORE molecular replacement program (CCP4, 1994), using the AChBP pentamer (Brejč et al., 2001) as search model. The structures were rebuilt in O (Jones et al., 1991) and refined with REFMAC (CCP4, 1994). TLS refinement, defining each subunit as a domain, was essential. For all structures a tight restraint on noncrystallographic symmetry (NCS) was absolutely required to improve refinement, indicating that data were not of high quality. Residues in loop C (180–194) and loop F (151–164) were excluded from NCS restraints because of variability in main chain and side chain orientation between the subunits. At the end of refinement, other parts of the structure were relieved from NCS restraints (see PDB files for details). To diminish the effect of model bias, nicotine and carbamylcholine were positioned in the density at the final stages of refinement. Water molecules were found using the ARP/WARP program (CCP4, 1994) in combination with REFMAC cycles. Optimized multiple superposition was obtained with LSQMAN. Structure analysis was performed with Escet (Schneider, 2002) and CCP4 programs (CCP4, 1994).

#### Isothermal Titration Calorimetry

Isothermal titration calorimetry (ITC) experiments were performed with the VP-ITC MicroCalorimeter (MicroCal, Inc.) at 22°C. Recombinant AChBP purified from Sf9 insect cells was used in all ITC experiments described. Stock solutions of AChBP were prepared by dialysis against the appropriate buffer (25 mM buffer [pH 8.0], 100 mM NaCl) at 4°C o/n and diluted to 2, 3, and 8 μM for binding to nicotine, acetylcholine, and carbamylcholine, respectively. Nicotine (0.1 mM), acetylcholine chloride (0.1 mM), and carbamylcholine chloride (0.35 mM) were solubilized in the same buffer. Titration experiments of ligand into buffer alone were performed to determine the change in enthalpy (ΔH) caused by dilution. This background was subtracted from ΔH obtained from ligand-AChBP binding experiments. Corrected data were analyzed using software supplied by the ITC manufacturer to calculate association and dissociation constant (K<sub>a</sub> and K<sub>d</sub>, respectively) and stoichiometry (N). These parameters were obtained for a model describing one set of binding sites, using nonlinear least-squares fitting. Models with multiple (cooperative) binding sites were applied as well but were not successful in optimizing fitting parameters to any meaningful value.

#### Acknowledgments

We thank Puck Knipscheer for assistance in baculovirus expression, René van Elk for ligand binding experiments, John Ladbury for discussion of ITC data, Huub Kooyman for CSD analysis, Roel van der Schors for mass spectrometry, Anastassis Perrakis for discussion, ESRF synchrotron staff for data collection assistance, S.T.W. for support, and J.R.F. for initial support. The structures have been

deposited in the PDB with access codes 1UX2 (HEPES), 1UW6 (Nicotine), and 1UV6 (Carbamylcholine).

Received: October 10, 2003

Revised: December 19, 2003

Accepted: January 29, 2004

Published: March 24, 2004

#### References

- Abreo, M.A., Lin, N.H., Garvey, D.S., Gunn, D.E., Hettinger, A.M., Wasicak, J.T., Pavlik, P.A., Martin, Y.C., Donnelly-roberts, D.L., Anderson, D.J., et al. (1996). Novel 3-Pyridyl ethers with subnanomolar affinity for central neuronal nicotinic acetylcholine receptors. *J. Med. Chem.* 39, 817–825.
- Arias, H.R. (2000). Localization of agonist and competitive antagonist binding sites on nicotinic acetylcholine receptors. *Neurochem. Int.* 36, 595–645.
- Brejč, K., van Dijk, W.J., Klaassen, R.V., Schuurmans, M., van Der Oost, J., Smit, A.B., and Sixma, T.K. (2001). Crystal structure of an ACh-binding protein reveals the ligand-binding domain of nicotinic receptors. *Nature* 411, 269–276.
- CCP4 (Collaborative Computational Project 4) (1994). The CCP4 suite: programs for protein crystallography. *Acta Crystallogr. D* 50, 760–763.
- Cohen, J.B., Sharp, S.D., and Liu, W.S. (1991). Structure of the agonist-binding site of the nicotinic acetylcholine receptor. [3H]acetylcholine mustard identifies residues in the cation-binding subsite. *J. Biol. Chem.* 266, 23354–23364.
- Corringer, P.J., Le Novère, N., and Changeux, J.P. (2000). Nicotinic receptors at the amino acid level. *Annu. Rev. Pharmacol. Toxicol.* 40, 431–458.
- Cromer, B.A., Morton, C.J., and Parker, M.W. (2002). Anxiety over GABA(A) receptor structure relieved by AChBP. *Trends Biochem. Sci.* 27, 280–287.
- Damle, V.N., and Karlin, A. (1980). Effects of agonists and antagonists on the reactivity of the binding site disulfide in acetylcholine receptor from *Torpedo californica*. *Biochemistry* 19, 3924–3932.
- Galzi, J.L., Bertrand, D., Devillers-Thierry, A., Revah, F., Bertrand, S., and Changeux, J.P. (1991). Functional significance of aromatic amino acids from three peptide loops of the alpha 7 neuronal nicotinic receptor site investigated by site-directed mutagenesis. *FEBS Lett.* 294, 198–202.
- Glennon, R.A., and Dukat, M. (2000). Central nicotinic receptor ligands and pharmacophores. *Pharm. Acta Helv.* 74, 103–114.
- Hansen, S.B., Radic, Z., Talley, T.T., Molles, B.E., Deerinck, T., Tsigelny, I., and Taylor, P. (2002). Tryptophan fluorescence reveals conformational changes in the acetylcholine binding protein. *J. Biol. Chem.* 277, 41299–41302.
- Harel, M., Kasher, R., Nicolas, A., Guss, J.M., Balass, M., Fridkin, M., Smit, A.B., Brejč, K., Sixma, T.K., Katchalski-Katzir, E., et al. (2001). The binding site of acetylcholine receptor as visualized in the X-ray structure of a complex between alpha-bungarotoxin and a mimotope peptide. *Neuron* 32, 265–275.
- Jones, T.A., Zou, J.Y., Cowan, S.W., and Kjeldgaard (1991). Improved methods for building protein models in electron density maps and the location of errors in these models. *Acta Crystallogr. A* 47, 110–119.
- Karlin, A. (2002). Emerging structure of the nicotinic acetylcholine receptors. *Nat. Rev. Neurosci.* 3, 102–114.
- Le Novère, N., and Changeux, J.P. (2001). The ligand gated ion channel database: an example of a sequence database in neuroscience. *Philos. Trans. R. Soc. Lond. B Biol. Sci.* 356, 1121–1130.
- Le Novère, N., Grutter, T., and Changeux, J.P. (2002). Models of the extracellular domain of the nicotinic receptors and of agonist- and Ca<sup>2+</sup>-binding sites. *Proc. Natl. Acad. Sci. USA* 99, 3210–3215.
- Martin, M., Czajkowski, C., and Karlin, A. (1996). The contributions of aspartyl residues in the acetylcholine receptor gamma and delta subunits to the binding of agonists and competitive antagonists. *J. Biol. Chem.* 271, 13497–13503.

- Middleton, R.E., and Cohen, J.B. (1991). Mapping of the acetylcholine binding site of the nicotinic acetylcholine receptor: [<sup>3</sup>H]nicotine as an agonist photoaffinity label. *Biochemistry* 30, 6987–6997.
- Miyazawa, A., Fujiyoshi, Y., and Unwin, N. (2003). Structure and gating mechanism of the acetylcholine receptor pore. *Nature* 424, 949–955.
- O'Leary, M.E., and White, M.M. (1992). Mutational analysis of ligand-induced activation of the *Torpedo* acetylcholine receptor. *J. Biol. Chem.* 267, 8360–8365.
- Osaka, H., Sugiyama, N., and Taylor, P. (1998). Distinctions in agonist and antagonist specificity conferred by anionic residues of the nicotinic acetylcholine receptor. *J. Biol. Chem.* 273, 12758–12765.
- Otwinowski, Z., and Minor, W. (1997). Processing of x-ray data collected in oscillation mode. In *Methods in Enzymology*, Volume 276, C.W. Carter, Jr., and R.M. Sweet, eds. (New York: Academic Press).
- Parker, M.J., Harvey, S.C., and Luetje, C.W. (2001). Determinants of agonist binding affinity on neuronal nicotinic receptor beta subunits. *J. Pharmacol. Exp. Ther.* 299, 385–391.
- Prince, R.J., and Sine, S.M. (1996). Molecular dissection of subunit interfaces in the acetylcholine receptor. Identification of residues that determine agonist selectivity. *J. Biol. Chem.* 271, 25770–25777.
- Reeves, D.C., and Lummis, S.C. (2002). The molecular basis of the structure and function of the 5-HT<sub>3</sub> receptor: a model ligand-gated ion channel (review). *Mol. Membr. Biol.* 19, 11–26.
- Schapira, M., Abagyan, R., and Totrov, M. (2002). Structural model of nicotinic acetylcholine receptor isotypes bound to acetylcholine and nicotine. *BMC Struct. Biol.* 2, 1.
- Schneider, T.R. (2002). A genetic algorithm for the identification of conformationally invariant regions in protein molecules. *Acta Crystallogr. D Biol. Crystallogr.* 58, 195–208.
- Sine, S.M. (2002). The nicotinic receptor ligand binding domain. *J. Neurobiol.* 53, 431–446.
- Sine, S.M., Quiram, P., Papanikolaou, F., Kreienkamp, H.J., and Taylor, P. (1994). Conserved tyrosines in the alpha subunit of the nicotinic acetylcholine receptor stabilize quaternary ammonium groups of agonists and curariform antagonists. *J. Biol. Chem.* 269, 8808–8816.
- Sixma, T.K., and Smit, A.B. (2003). Acetylcholine binding protein (AChBP): a secreted glial protein that provides a high-resolution model for the extracellular domain of pentameric ligand-gated ion channels. *Annu. Rev. Biophys. Biomol. Struct.* 32, 311–334.
- Smit, A.B., Syed, N.I., Schaap, D., van Minnen, J., Klumperman, J., Kits, K.S., Lodder, H., van der Schors, R.C., van Elk, R., Sorgedraeger, B., et al. (2001). A glia-derived acetylcholine-binding protein that modulates synaptic transmission. *Nature* 411, 261–268.
- Taylor, R., and Kennard, O. (1982). Crystallographic evidence for the existence of C-H-O, C-H-N, and C-H-Cl hydrogen bonds. *J. Am. Chem. Soc.* 104, 5063–5070.
- Unwin, N., Miyazawa, A., Li, J., and Fujiyoshi, Y. (2002). Activation of the nicotinic acetylcholine receptor involves a switch in conformation of the alpha subunits. *J. Mol. Biol.* 319, 1165–1176.
- Vafa, B., and Schofield, P.R. (1998). Heritable mutations in the glycine, GABAA, and nicotinic acetylcholine receptors provide new insights into the ligand-gated ion channel receptor superfamily. *Int. Rev. Neurobiol.* 42, 285–332.
- Xie, Y., and Cohen, J.B. (2001). Contributions of *Torpedo* nicotinic acetylcholine receptor gamma Trp-55 and delta Trp-57 to agonist and competitive antagonist function. *J. Biol. Chem.* 276, 2417–2426.
- Zhong, W., Gallivan, J.P., Zhang, Y., Li, L., Lester, H.A., and Dougherty, D.A. (1998). From ab initio quantum mechanics to molecular neurobiology: a cation-pi binding site in the nicotinic receptor. *Proc. Natl. Acad. Sci. USA* 95, 12088–12093.